Catalysis Today 171 (2011) 150–155

Contents lists available at ScienceDirect

Catalysis Today

journal homepage: www.elsevier.com/locate/cattod

Marked role of mesopores for the prevention of sintering and carbon deposition in dry reforming of methane over ordered mesoporous Ni–Mg–Al oxides

Weihua Shen, Hideaki Momoi, Kenta Komatsubara, Taiga Saito, Akihiro Yoshida, Shuichi Naito*

Department of Material and Life Chemistry, Kanagawa University, 3-27-1, Rokkakubashi, Kanagawa-ku, Yokohama, 221-8686, Japan

ARTICLE INFO

Article history:
Received 30 October 2010
Received in revised form 21 February 2011
Accepted 1 April 2011
Available online 8 May 2011

Keywords:
Mesoporous
Ni–Mg–Al oxides
Dry reforming
CH_4
CO_2

ABSTRACT

Ordered mesoropous Ni–Al and Ni–Mg–Al oxides were prepared by evaporation induce self-assembly method using Pluronic P123 as a soft template. Ni–Al and Ni–Mg–Al oxides without P123 addition were also prepared. The prepared ordered mesoporous catalysts showed much higher activity and durability for dry reforming of methane than those without ordered mesoporous structure. The N_2 sorption and transmission electron microscope observation revealed that the ordered structure was kept after reaction at 750 °C for 30 h. The sintering of Ni was prevented and the coke formation was suppressed on mesoporous catalysts. Although the addition of Mg was not so efficient for improving the activity of mesoporous catalyst, benefit for suppressing coke formation was observed.

1. Introduction

Dry reforming of methane to produce synthesis gas has attracted very much attention during the past decades. Two kinds of greenhouse gases, methane and carbon dioxide, can be consumed by this reaction to give synthesis gas with high CO/H_2 ratio, which is desirable for the synthesis of long-chain hydrocarbon in Fischer–Tropsch reaction. Beside noble metals such as Ru [1] and Rh [2], Ni metal was found to exhibit high catalytic activity for this reaction. Various oxides, such as SiO_2 [3], MgO [4], Al_2O_3 [5–7], ZrO_2 [8], and Mg–Al oxides [9–12] have been reported as supports for Ni metal. Among them, considerable amounts of the previous reports utilized Al_2O_3 and Mg–Al oxides as Ni support because of their high thermal-stability. The major drawback of nickel catalyst for dry reforming of methane is the rapid deactivation caused by the carbon deposition and Ni sintering.

It has been reported that a high dispersion of the metallic Ni over supports could limit the coke formation [13,14]. Mesoporous materials prepared from surfactant assistant assembly have ordered structure, high surface areas, and narrow pore-size distribution [15]. Those features make mesoporous materials to be a good support for preventing metal particle from sintering [16,17]. After a reliable and reproducible preparation method for ordered mesoporous alumina was reported by Yuan et al. [18], we extended their method to the preparation of tri-compound Ni–Mg–Al oxides with ordered mesoporous structure and examined their catalytic performance for the steam reforming of methane. We found that the formation of coke and the Ni sintering was suppressed using ordered mesoporous Ni–Mg–Al oxides as catalyst during the catalytic steam reforming of methane [19].

In the present report, we investigated the catalytic performance of ordered mesoporous Ni–Mg–Al oxides for dry reforming of methane to clarify the role of mesopores in the prevention of Ni sintering and inactive carbon deposition during reaction. The catalysts before and after reaction were characterized by small and wide-angle X-ray diffraction (XRD), Transmission electron microscope (TEM), thermal gravity (TG) and N_2 sorption.

2. Experimental

2.1. Preparation of catalysts

The preparation method of ordered mesoporous Ni–Mg–Al oxides was the same as our previous reports [19]. The added amount of NiO was fixed to 10 wt% (about 7 wt% of Ni after reduction), and the molar ratio of Mg/(Mg + Al) was 0%, and 20 mol% (named as Ni/MA and Ni/20MgMA, respectively, where MA indicates mesoporous alumina). For preparation of Ni/MA, 1 g of surfactant Pluronic P123 was dissolved in 20 mL ethanol. 2.04 g of $Al(O\text{–}Pr\text{–}i)_3$ (10 mmol), 0.224 g of $Ni(NO_3)_2{\cdot}6H_2O$, and 1.70 mL of 60% HNO_3 (22 mmol), was added to the P123 solution under stirring. The mixture was continued to stir for 5 h to obtain a clear solution. The solution was then put into 60 °C oven for 48 h in order to evaporate EtOH for 4 h. Finally, the obtained solid product was

* Corresponding author. Tel.: +81 45 481 5661, fax: +81 45 413 9770.
E-mail address: naitos01@kanagawa-u.ac.jp (S. Naito).

0920-5861/$ – see front matter © 2011 Elsevier B.V. All rights reserved.
doi:10.1016/j.cattod.2011.04.003

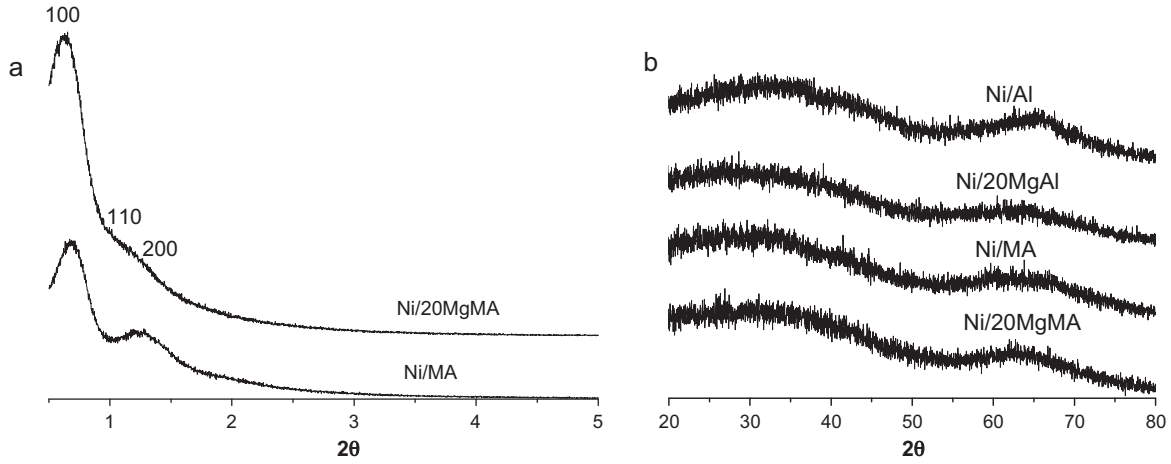

Fig. 1. (a) Small-angle, and (b) wide-angle XRD patterns of as-prepared catalysts.

calcined at 500 °C for 4 h to remove the surfactant P123. For preparation of Ni/20MgMA, 1 g of P123 was dissolved in 20 mL ethanol. 1.63 g of Al(O–Pr–i)$_3$ (8 mmol), 0.52 g of Mg(NO$_3$)$_2$·6H$_2$O (2 mmol), 0.213 g of Ni(NO$_3$)$_2$·6H$_2$O, and 1.24 mL of 60% HNO$_3$ (16 mmol) was added to the P123 solution under stirring. Other processes were the same as the preparation of Ni/MA. The obtained samples were ground to powder before characterizations or catalytic tests.

To compare the catalytic property, Ni–Al oxides and Ni–Mg–Al oxides without ordered mesopore were also prepared. The preparations of these two catalysts (named as Ni/Al for Ni–Al oxide and Ni/20MgAl for Ni–Mg–Al oxide) were similar to Ni/MA, and Ni/20MgMA, respectively, just without the addition of surfactant.

2.2. Characterization of catalysts

Wide-angle XRD patterns were recorded on Rigaku MultiFlex 2KW using Cu Kα1 source operated at 40 kV and 20 mA. Small-angle XRD patterns were recorded on Rigaku RINT-Ultima III using CuKα1 source with 40 kV and 40 mA. TEM observation was performed on JEOL JEM-2010 with 200 kV accelerating voltage. N_2 sorption measurement was carried out on Micromeritics Tristar 3000 at liquid nitrogen temperature. Prior to N_2 sorption measurement, the sample was degassed in vacuum at 250 °C for 1 h. The specific surface area was calculated by the Brunauer-Emmett-Teller (BET) method. The TG measurement (conducted on Rigaku Thermo Plus, TG 8120) was adopted to estimate the amount of deposited carbon after 30 h reaction. About 8 mg of spent sample was put into a Pt pan under 25% O_2/He gas-flow and the temperature was increased from room temperature to 900 °C with a ramp rate of 10 °C/min; an online quadruple mass spectroscopy (QMS, Pfeiffer QME200) was utilized for the analysis of the outlet gas.

Temperature-programmed-reduction (H_2-TPR) measurements of catalysts were conducted on a gas-flow system to characterize the Ni reducibility. 300 mg of catalyst was equipped into a quartz tube furnace, and was pretreated with 50 mL/min of 10% O_2/He at 500 °C for 30 min. After the temperature cooling down to room temperature under He, 50 mL/min of 5% H_2/He was flowed for 10 min. Then the temperature was increased to 900 °C with a ramp rate of 10 °C/min under 50 mL/min of 5% H_2/He gas-flow. The outlet H_2 concentration was analyzed by the online QMS.

2.3. Procedure of catalytic reaction

The catalytic dry reforming of methane was performed on a fixed-bed-gas-flow system. Temperature dependence and steady-state durability experiments were carried out to evaluate the catalytic property of the prepared catalyst. Prior to each run, the catalysts were reduced by a mixed gas with composition of 5 mL/min of H_2 and 25 mL/min of N_2 at 750 °C for 30 min. A premixed gas with composition of 25 mL/min of CO_2, 25 mL/min of CH_4 and 35 mL/min of N_2 was used as the gas feed. The outlet gas was analyzed by an online gas chromatography (Agilent 3000A Microgc) equipped with Porapark Q and Molecular sieve 13X columns using TCD as detectors. For the experiments of the temperature dependence, a mixture of 10 mg catalyst and 290 mg quartz sand was used as the catalyst. The temperature of catalyst bed was measured by a sliding thermocouple dipped inside the catalyst bed, and catalytic activity was tested at the temperature from 500 °C to 750 °C. The durability experiments of catalysts were conducted at 750 °C for 30 h by the same gas feed as temperature dependence experiments, employing both 10 mg of catalyst with silica dilution and 150 mg of catalyst without silica dilution.

3. Results and discussion

The formation of hexagonal ordered mesoporous structures (P6 mm symmetry) was identified by small-angle XRD patterns as shown in Fig. 1a. The small-angle XRD patterns of Ni/MA, Ni/20MgMA exhibited a strong (1 0 0) peak and an overlapped peak assigned to (1 1 0) and (2 0 0), indicating the existence of ordered mesoporous structure. As shown in Fig. 1b, wide-angle XRD patterns of as-prepared Ni/Al, Ni/20MgAl, Ni/MA and Ni/20MgMA

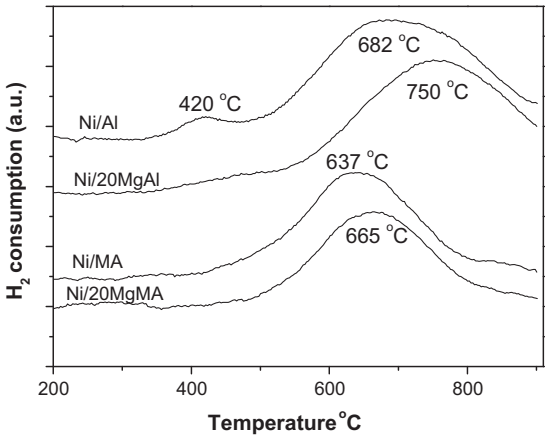

Fig. 2. H_2-TPR results of varied catalysts (300 mg of catalyst, 50 mL/min of 5% H_2/He, 10 °C/min).

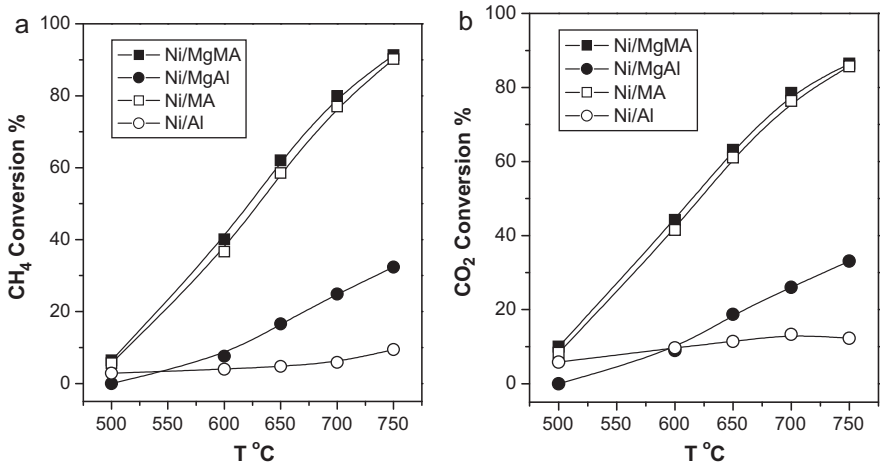

Fig. 3. Temperature dependences of (a) CH_4 and (b) CO_2 conversion on Ni/Al, Ni/20MgAl, Ni/MA and Ni/20MgMA catalysts during dry reforming of methane (10 mg catalyst, $CH_4/CO_2/N_2$ = 25/25/35 mL/min).

exhibited only very weak peaks corresponding to Al_2O_3, indicating the homogeneous dispersion of Mg and Ni in the samples.

The H_2-TPR has been utilized for the characterization of Ni reducibility in the prepared catalysts. The results were shown in Fig. 2. The weak peak at 420 °C on Ni/Al sample can be assigned to the reduction of big size NiO according to the literature [20]. The main peak at 682 °C on Ni/Al can be assigned to the highly dispersed NiO. With the addition of Mg, the reduction peak on Ni/20MgAl was shifted to higher temperature as 750 °C. On the other hand, the reduction peaks on Ni/MA and Ni/20MgMA are 637 °C and 665 °C, respectively, which are 50–100 °C lower than those on the samples without ordered mesoporous structure. The lowering of the reduction temperatures of Ni on mesoporous samples may be explained by the fact that the higher surface areas and abundant pore systems of the mesoporous samples facile the diffusion of H2 and the Ni from the framework to the pore surface. The reduction temperatures of Ni in Mg added Ni/20MgMA and Ni/20MgAl catalysts were higher than those on Ni/MA and Ni/Al, respectively. Although the XRD patterns showed that the as-prepared Ni/20MgAl and Ni/20MgMA was amorphous, some $MgAl_2O_4$ spinel unit might already be formed since spinel phase was observed on those two samples after H_2 reduction. The closed sizes of Ni^{2+} (0.69 Å) and Mg^{2+} (0.66 Å) cations allow Ni^{2+} get into the Mg^{2+} site forming spinel unit of $NiAl_2O_4$. It is well known that the reduction of Ni in spinel $NiAl_2O_4$ needs relatively high temperature [12].

Fig. 3 shows the results of temperature-dependence experiments over varied catalysts. The tendency of activity to temperature was the same for all the catalysts. The conversion of CH_4 and CO_2 was increased with the increase of the reaction temperature from 500 °C to 750 °C. The difference of the catalytic activity became obvious at the temperature above 600 °C. The conversions of CH_4 and CO_2 on mesoporous Ni/MA and Ni/20MgMA catalysts were much higher than those on Ni/Al and Ni/20MgAl, revealing much higher catalytic activity of mesoporous catalysts. The effect of Mg addition was also observed by comparing the conversions on Ni/Al and Ni/20MgAl. The conversion on Ni/20MgAl was higher than that on Ni/Al above 600 °C. The conversion on Ni/20MgMA was slightly higher than that on Ni/MA at each temperature. However, the effect of Mg addition was not comparable to the effect of mesopore.

The durability testes of the 10 mg catalyst diluted with 290 mg of quartz sand was carried out for the stability checking. As shown in Fig. 4a, the conversions of CH_4 on mesoporous catalysts are higher than those on the catalysts without ordered mesoporers at any time, indicating higher catalytic activity of the catalysts with mesopores. The conversions of methane on Ni/Al and Ni/20MgAl were decreased very quickly at the beginning 10 h (CH_4 conversion from 60% to 20% on Ni/20MgAl, and from 38% to 6% on Ni/Al), and then kept almost unchanged. On the other hand, the conver-

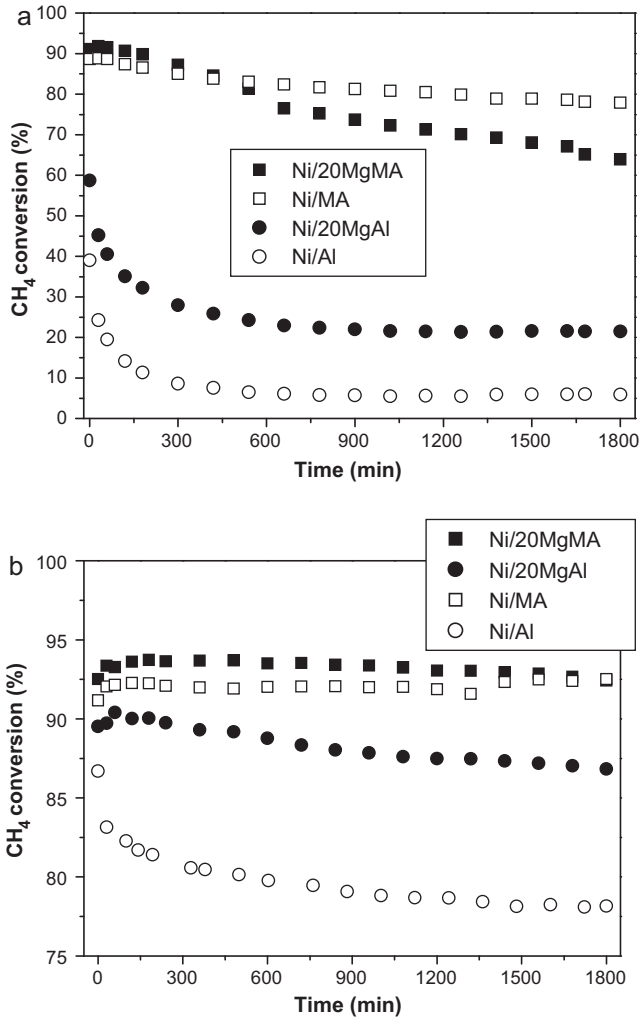

Fig. 4. CH_4 conversion on varied catalysts during methane dry reforming at 750 °C, using (a) 10 mg and (b) 150 mg of catalyst ($CH_4/CO_2/N_2$ 25/25/35 mL/min).

Table 1
The pore parameters of the catalysts after H_2 reduction, and after 30 h catalytic dry reforming of methane and catalytic results of the catalysts.

Catlysts	S_{BET} (m^2/g)		Pore V (cm^3/g)		Pore size D (nm[a])		CH_4 Conv.[b]	Coke[c]
	Aft. Red.	Aft. Rea.	Aft. Red.	Aft. Rea.	Aft. Red.	Aft. Rea.	at 750 °C%	
Ni/MA	177	171	0.535	0.523	12.3	11.2	92 (92)	Trace
Ni/20MgMA	169	121	0.593	0.442	14.0	13.6	93.5 (92)	No
Ni/Al	48	40	0.071	0.058	4.9	5.3	86 (78)	Trace
Ni/20MgAl	114	83	0.116	0.150	4.1	5.8	90 (86)	27%

Aft. Red. = After H_2 reduction. Aft. Rea. = After 30 h reaction.
[a]The most probable pore-size was calculated from the adsorption branch.
[b]The conversion of CH_4 on 150 mg of catalyst and in ( ) is that after 30 h reaction.
[c]The coke was estimated by TG and mass spectroscopy.

sions on Ni/20MgMA and Ni/MA were gradually decreased with the lapse of time (CH_4 conversion from 92% to 65% on Ni/20MgMA, and from 89% to 78% on Ni/MA). The conversion on Ni/20MgMA was higher than that on Ni/MA at the beginning, and was lower than that on Ni/MA after 10 h, suggesting the higher stability of Ni/MA than Ni/20MgMA. The Mg addition effect was obvious over Ni/Al and Ni/20MgAl since much higher conversion was observed on Ni/20MgAl than that on Ni/Al. However, the effect was not obvious on mesoporous catalyst by the comparison of conversions between Ni/MA and Ni/20MgMA.

In order to investigate the effect of W/F and to characterize the spent catalysts, 150 mg pure sample was also used as catalyst for the dry reforming of methane for 30 h reaction. As shown in Fig. 4b and summarized in Table 1, the activity order of the catalysts was as follows: Ni/20MgMA > Ni/MA > Ni/20MgAl > Ni/Al. The conversion of CH_4 on Ni/Al and Ni/20MgAl was gradually decreased during the 30 h reaction due to the deactivation. However, no deactivations were observed on Ni/MA and Ni/20MgMA, because of the excess amount of catalysts and the conversion of CH_4 was kept almost unchanged during 30 h reaction.

After 30 h catalytic dry reforming of methane, the purely spent catalysts were taken out and the deposited carbon was analyzed by TG with an online QMS. As shown in Fig. 5a, a weight increase corresponding to the oxidation of Ni was observed at 300–400 °C on all the samples. The weight loss on spent Ni/20MgAl was started from 500 °C and completed at 700 °C. Meanwhile, mass number (m/e = 44) corresponded to CO_2 was detected during this period. The weight loss was very small on the other three spent catalysts, indicating little carbon deposition. By the QMS analysis (Fig. 5b), CO_2 was undetected on spent Ni/20MgMA, and small amount CO_2 was detected on spent Ni/MA and Ni/Al. The outlet-CO_2 peak at 350 °C could be assigned to the active carbon deposited on Ni metal, which burned off during the Ni oxidation to NiO, and the amount of this active carbon on spent Ni/MA was more than that on spent Ni/Al. The outlet-CO_2 peak on Ni/Al at 650 °C can be assigned to the inert carbon.

From these experimental results, we could conclude that the ordered mesoporous structure can improve the coke resistance in dry reforming of methane, and the Mg addition in mesoporous catalyst can even more suppress the coke formation. However, no obvious relationship was observed between the amount of carbon and the catalytic activity during the durability test. Although trace of carbon was deposited on Ni/Al catalyst and large amount of carbon was deposited on Ni/20MgAl, the activity of Ni/Al was much poorer than that of Ni/20MaAl (see Fig. 4). Similar conclusion has been drawn by Quek et al. [21]. They found that a mesoporous Ni/SiO_2, prepared by impregnation method, although without carbon deposition, showed much poorer activity and stability in dry reforming of methane than the other two mesoporous Ni/SiO_2 catalysts (prepared by Ni-grafted and direct incorporation methods) which really formed considerable amount of carbon. For Ni/MA and Ni/20MgMA catalysts, the negligible carbon deposition implied that the deactivations of both catalysts were not responded to the carbon deposition, but caused from textural-morphology change and/or Ni sintering.

To investigate the textural change, N_2 sorption was carried out on the catalysts before and after reaction. Fig. 6 shows the N_2 sorption isotherms and pore size distributions of the catalysts after H_2 reduction and after 30 h reaction, and their pore parameters were summarized in Table 1. Both the N_2 sorption isotherms of Ni/MA and Ni/20MgMA after H_2 reduction are typical type IV sorption isotherms with H1 hysteresis loops, which are characteristic for

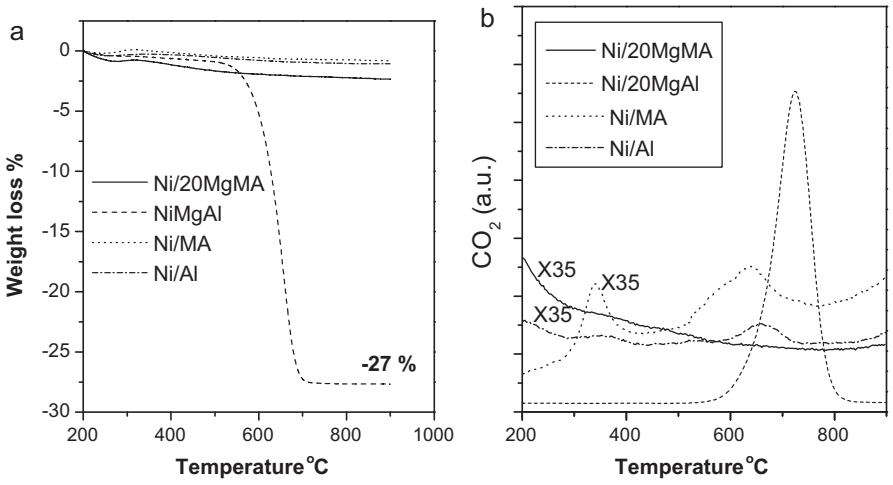

Fig. 5. (a) TG profiles and (b) intensity of CO_2 (detected by mass spectroscopy with m/e = 44) formation during TG measurement. (8 mg of spent catalyst, 200 mL/min 25% O_2/He, from room temperature to 900 °C with a ramp rate of 10 °C/min).

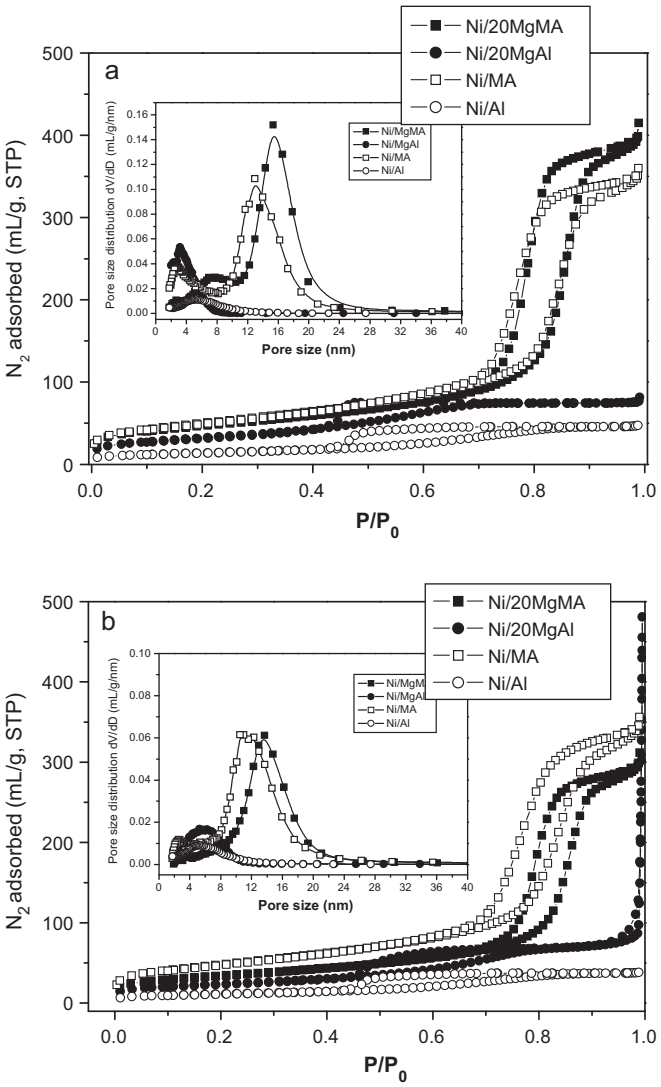

Fig. 6. The isotherms of N_2 adsorption–desorption at 77 K and the corresponding pore size distribution (inset) for (a) the catalysts after H_2 reduction, and (b) the catalysts after 30 h catalytic dry reforming of methane.

mesoporous materials with cylinder pores, suggesting the mesoporous structure was remained after H_2 reduction. The pore size distribution (Fig. 6a inset) shows the narrow pore size distributions of the ordered mesoporous catalysts Ni/MA and Ni/20MgMA. Although the isotherms and pore distributions (Fig. 6b) of spent Ni/MA and Ni/20MgMA were similar to those before reaction, the specific BET surface areas and pore volumes of the spent catalysts are decreased to some extent after 30 h reaction (see Table 1). The reason for higher durability of Ni/MA than Ni/20MgMA may be the higher stability of Ni/MA than Ni/20MgMA (the surface area of spent Ni/MA was higher than spent Ni/20MgMA).

To explore the effect of the Ni metal particle size, XRD and TEM observation were conducted on the catalysts before and after reaction. The XRD patterns of the catalysts after H_2 reduction and after catalytic dry reforming of methane are shown in Fig. 7. The XRD patterns of Ni/Al and Ni/MA showed the Al_2O_3 phase was changed from amorphous to γ-Al_2O_3 after H_2 reduction and the crystalline was a little increased after dry reforming of methane. For Ni/20MgAl and Ni/20MgMA, a crystallized $MgAl_2O_4$ spinel phase was detected after H_2 reduction, and the intensity of the diffraction peak for both case were increased after catalytic dry reforming of methane. The metallic Ni (2 0 0) peaks of Ni/MA and Ni/20MgMA catalysts were almost invisible after H_2 reduction, suggesting the existence of highly dispersed Ni nano-particles. Although the Ni (2 0 0) peaks of Ni/MA and Ni/20MgMA were observed after reaction, the reflection peaks were still weaker and broader than those of non-mesoporous catalysts, suggesting that the mesopore can prevent the metallic Ni nano-particle from severe sintering.

The TEM images of Ni/20MgMA and Ni/20MgAl after H_2 reduction and after dry reforming of methane are shown in Fig. 8. The presence of uniform and hexagonal ordered mesopores with *P6mm* symmetry was confirmed by the TEM observation. The typical TEM image of well ordered hexagonal mesoporous structure along (0 0 1) direction was observed on Ni/20MgMA sample. The metallic Ni particle-sizes on Ni/20MgMA were 3–5 nm after H_2 reduction. The TEM observation revealed the Ni particle-size of mesoporous catalyst was increased to 5–10 nm after dry reforming of methane, and the ordered mesoporous structure was maintained. No deposited carbon was observed on spent Ni/20MgMA. On the other hand, in the case of Ni/20MgAl catalyst, the TEM images imply the Ni particles severely sintered during H_2 reduction. The Ni particle-size of Ni/20MgAl after H_2 reduction was broadly distributed from 3 nm to 30 nm. The main coke on spent Ni/20MgAl observed by TEM was filament carbons including nano-fibers and nano-tubes. Amorphous carbon covering bigger sizes of Ni was also observed.

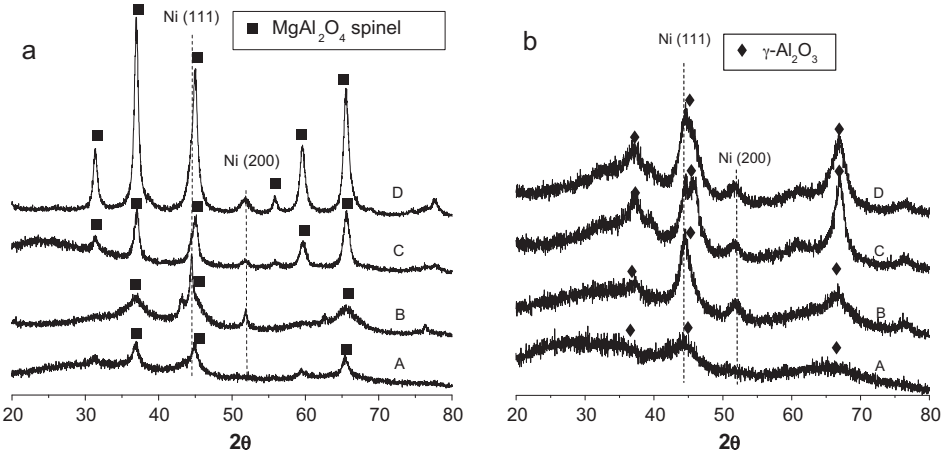

Fig. 7. XRD patterns of (a) Ni/20MgMA after H_2 reduction (A), Ni/20MgAl after H_2 reduction (B), Ni/20MgMA after 30 h reaction (C), and Ni/20MgAl after 30 h reaction (D); and (b) Ni/MA after H_2 reduction (A), Ni/Al after H_2 reduction (B), Ni/MA after 30 h reaction (C), and Ni/Al after 30 h reaction (D).

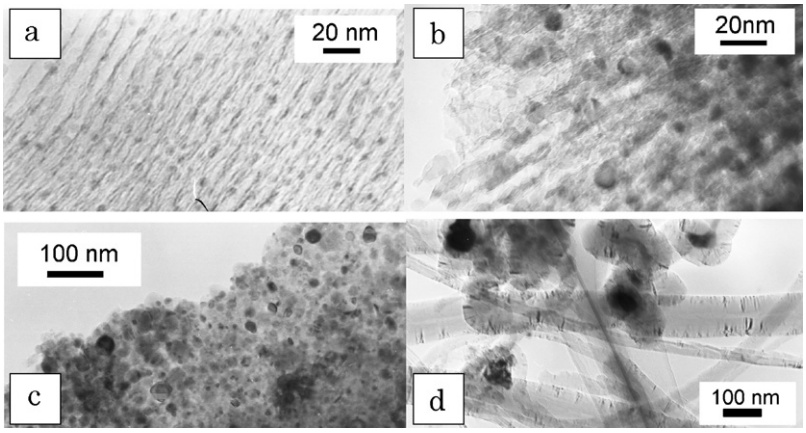

Fig. 8. TEM images of (a) Ni/20MgMA after H_2 reduction at 750 °C, (b) Ni/20MgMA after 30 h reaction, (c) Ni/20MgAl after H_2 reduction at 750 °C, (d) Ni/20MgAl after 30 h reaction.

As we have reported previously, the pore of Ni/Al and Ni/20MgAl, mainly was micropore, was formed from the decomposition of remained nitrate [19]. There are also micropores on Ni/MA and Ni/20MgMA, which are formed from removal of the PEO chain imbedded in the wall of mesopore or from decomposition of nitrate. As being confirmed by XRD, crystallization takes place during the H_2 reduction and/or methane dry reforming at relatively high temperature, which eliminates the micropores and causes the shrinkage of the structure and the decrease of surface area and pore size. However, for Ni/MA and Ni/20MgMA, considerable extent of ordered mesopores can be maintained even after 30 h reaction. The Ni particles confined in mesopores can move only along the pore direction, resulting in the prevention of Ni from severe-sintering and limitation of coke formation. On the other hand, the unconfined Ni particles on non-mesoporous catalysts can move along the support surface 2-dimensionally, resulting in severe sintering and causing the fast deactivation of non-mesoporous catalysts during reaction (Fig. 4a). Combining the results of catalytic reaction and the characterizations of the catalysts, it is clear that smaller Ni particle is more beneficial to the catalytic activity for dry reforming of methane.

4. Conclusion

We have succeeded in the preparation of tri-component ordered mesoporous Ni–Mg–Al oxides, which have high surface area and pore volume. The existence of ordered mesoporous structure can decrease the Ni reduction temperature for 50–100 °C. The ordered mesoporous Ni–Al oxides and Ni–Mg–Al oxides show higher catalytic activity for methane dry reforming reaction than those without ordered meoporous structure. The N_2 sorption measurements and TEM images demonstrated that the ordered mesoporous structure can be maintained after 30 h reaction at 750 °C. The ordered mesoporous structure can improve the coke resistance in methane dry reforming, and the Mg addition can even more suppress the coke formation. The role of mesopores is the prevention of metallic Ni particles from severe sintering and the promotion of the coke resistance during the reaction.

References

[1] L. Paturzo, F. Gallucci, A. Basile, G. Vitulli, P. Pertici, Catal. Today 82 (2003) 57.
[2] P. Gronchi, P. Centola, R. Del Rosso, Appl. Catal., A 152 (1997) 83.
[3] J. Nakamura, K. Aikawa, K. Sato, T. Uchijima, Catal. Lett. 25 (1994) 265.
[4] F. Frusteri, F. Arena, G. Calogero, T. Torre, A. Parmaliana, Catal. Commun. 2 (2001) 49.
[5] U. Olsbye, T. Wurzel, L. Mleczko, Ind. Eng. Chem. Res. 36 (1997) 5180.
[6] Z. Cheng, Q. Wu, J. Li, Q. Zhu, Catal. Today 30 (1996) 147.
[7] T. Osaki, T. Mori, J. Catal. 204 (2001) 89.
[8] M. Rezaei, S. Mahdi Alavi, S. Sahebdelfar, L. Xinmei, L. Qian, Z. Yan, Energy Fuels 21 (2007) 581.
[9] A.I. Tsyganok, T. Tsunoda, S. Hamakawa, K. Suzuki, K. Takehira, T. Hayakawa, J. Catal. 213 (2003) 191.
[10] T. Shishido, M. Sukenobu, H. Morioka, R. Furukawa, H. Shirahase, K. Takehira, Catal. Lett. 73 (2001) 21.
[11] C.E. Daza, J. Gallego, F. Mondragon, S. Morena, R. Molina, Fuel 89 (2010) 592.
[12] J. Guo, H. Lou, H. Zhao, D. Chai, X. Zheng, Appl. Catal., A 273 (2004) 75.
[13] J.R. Rostrup-Nielsen, J. Sehested, J.K. Norskov, Adv. Catal. 47 (2002) 65.
[14] D. Chen, K.O. Christensen, E. Ochoa-Fernández, Z. Yu, B. Tøtdal, N. Latorre, A. Mnzón, A. Holmen, J. Catal. 229 (2005) 82.
[15] D. Zhao, Q. Huo, J. Feng, B.F. Chmelka, G.D. Stucky, J. Am. Chem. Soc. 120 (1998) 6024.
[16] A. Fukuoka, H. Araki, J. Kimura, Y. Sakamoto, T. Higuchi, N. Sugimoto, S. Inagaki, M. Ichikawa, J. Mater. Chem. 14 (2004) 752.
[17] L. Li, J.-L. Shi, J.-N. Yan, Chem. Commun. (2004) 1990.
[18] Q. Yuan, A.-X. Yin, C. Luo, L.-D. Sun, Y.-W. Zhang, W.-T. Duan, H.-C. Liu, C.-H. Yan, J Am. Chem. Soc. 130 (2008) 3465.
[19] W. Shen, K. Komatsubara, T. Hagiyama, A. Yoshida, S. Naito, Chem. Commun. (2009) 6490.
[20] K.Y. Koo, H.-S. Roh, U.H. Jung, W.L. Yoon, Catal. Lett. 130 (2009) 217.
[21] X.-Y. Quek, D. Liu, W.N.E. Cheo, H. Wang, Y. Chen, Y. Yang, Appl. Catal., B 95 (2010) 374.